JCS ePress online publication date 8 June 2010

Phosphorylation regulates polarisation of chitin synthesis in *Candida albicans*

Megan D. Lenardon[1], Sarah A. Milne[1], Héctor M. Mora-Montes[1], Florian A. R. Kaffarnik[2,*], Scott C. Peck[3], Alistair J. P. Brown[1], Carol A. Munro[1] and Neil A. R. Gow[1,‡]

[1]School of Medical Sciences, Institute of Medical Sciences, University of Aberdeen, Foresterhill, Aberdeen, AB25 2ZD, Scotland, UK
[2]The Sainsbury Laboratory, Norwich Research Park, Colney Lane, Norwich, NR4 7UH, UK
[3]Division of Biochemistry, 271H Bond Life Sciences Center, University of Missouri-Columbia, Columbia, MO 65211, USA
*Present address: Department of Botany, Technical University of Darmstadt, Schnittspahnstrasse 6, Darmstadt, Germany
‡Author for correspondence (n.gow@abdn.ac.uk)

Accepted 6 April 2010
Journal of Cell Science 123, 2199-2206
© 2010. Published by The Company of Biologists Ltd
doi:10.1242/jcs.060210

Summary

The ability to undergo polarised cell growth is fundamental to the development of almost all walled organisms. Fungi are characterised by yeasts and moulds, and both cellular forms have been studied extensively as tractable models of cell polarity. Chitin is a hallmark component of fungal cell walls. Chitin synthesis is essential for growth, viability and rescue from many conditions that impair cell-wall integrity. In the polymorphic human pathogen *Candida albicans*, chitin synthase 3 (Chs3) synthesises the majority of chitin in the cell wall and is localised at the tips of growing buds and hyphae, and at the septum. An analysis of the *C. albicans* phosphoproteome revealed that Chs3 can be phosphorylated at Ser139. Mutation of this site showed that both phosphorylation and dephosphorylation are required for the correct localisation and function of Chs3. The kinase Pkc1 was not required to target Chs3 to sites of polarised growth. This is the first report demonstrating an essential role for chitin synthase phosphorylation in the polarised biosynthesis of fungal cell walls and suggests a new mechanism for the regulation of this class of glycosyl-transferase enzyme.

Key words: Chitin, Cell wall, *Candida albicans*, Chs3, Pkc1, Phosphorylation, Polarised growth

Introduction

Chitin is nature's second-most abundant polymer after cellulose, but the regulation of its synthesis is poorly understood. It is an essential component of the cell wall of all pathogenic fungi, as well as occurring in the cyst walls of pathogenic amoebae, the eggshells and gut lining of parasitic nematodes, and the exoskeletons of invertebrate vectors of human disease. Chitin synthesis is essential for growth, development and viability in fungi and insects, and can rescue fungi from otherwise lethal cell-wall stresses (Merzendorfer, 2006; Munro and Gow, 2001; Roncero, 2002; Walker et al., 2008). A detailed understanding of the mechanics of chitin synthesis might facilitate the generation of specific inhibitors with broad utility in the treatment of human and plant diseases.

Fungi typify many eukaryotic cell types exhibiting highly polarised cell growth. The polarised expansion of the walls of buds and hyphae of fungi has been studied extensively as a general model for polarised cell-wall biosynthesis (for a review, see Fischer et al., 2008). Fungal chitin synthesis is an essential process in most fungi, and is under tight spatial and temporal regulation. In the polymorphic human fungal pathogen *Candida albicans*, chitin synthesis is achieved by four chitin synthase isoenzymes, Chs1, Chs2, Chs3 and Chs8, each with individual but sometimes overlapping functions (Bulawa et al., 1995; Gow et al., 1994; Lenardon et al., 2007; Mio et al., 1996; Munro et al., 2003; Munro et al., 2001; Walker et al., 2008). *C. albicans* chitin synthases are regulated at both transcriptional and post-transcriptional levels. The *CHS* genes are regulated differentially during yeast and hyphal growth and during the cell cycle (Munro et al., 1998; Munro et al., 2003; Sudoh et al., 1993). However, changes in chitin synthase activity (Chs2 and Chs8) do not always parallel mRNA levels, indicating that additional regulation occurs at the post-transcriptional level (Munro and Gow, 2001; Munro et al., 1998). *CHS* genes are also transcriptionally activated in response to various stresses (Munro et al., 2007; Walker et al., 2008), but recent analyses of the promoters of the class I *CHS* genes (*CHS2* and *CHS8*) suggest that post-transcriptional regulation plays a more dominant role in directing chitin synthesis in *C. albicans* (Lenardon et al., 2009). Several post-transcriptional regulatory mechanisms have been suggested to modulate chitin synthesis (Choi et al., 1994; Chuang and Schekman, 1996; Martinez-Rucobo et al., 2009; Munro and Gow, 2001; Munro et al., 1998; Roncero, 2002; Valdivia and Schekman, 2003).

The class IV chitin synthases (Chs3) of *Saccharomyces cerevisiae* (*Sc*) and *C. albicans* (*Ca*) synthesise the majority of the chitin found in the cell wall, as well as the chitin ring at bud sites (Bulawa et al., 1995; Mio et al., 1996). *Ca*Chs3 is required for the formation of short chitin rodlets in the cell wall, and *Ca*Chs3-YFP is localised at the tip of growing buds and hyphae, and relocates to the site of septum formation just before cytokinesis (Lenardon et al., 2007). Export of *Sc*Chs3 from the endoplasmic reticulum (ER) is controlled by the chaperone *Sc*Chs7 (Trilla et al., 1999). A large complex that includes the essential components *Sc*Chs5 and *Sc*Chs6, as well as *Sc*Bch1, *Sc*Bch2 and *Sc*Bud7, transports *Sc*Chs3 from the Golgi apparatus to the plasma membrane (PM) (Sanchatjate and Schekman, 2006; Santos and Snyder, 1997; Trautwein et al., 2006; Ziman et al., 1996; Ziman et al., 1998). *Sc*Chs3 is transported in secretory vesicles called chitosomes (Bartnicki-Garcia, 2006; Chuang and Schekman, 1996; Santos and Snyder, 1997; Ziman et al., 1996).

Protein and lipid phosphorylation play a number of roles in the regulation of chitin synthesis in *S. cerevisiae*. Phosphorylation of

*Sc*Chs3 in response to heat stress is dependent on *Sc*Pkc1 (Valdivia and Schekman, 2003). *Sc*Chs3 forward transport is inhibited by the deletion of *Sc*Sac1 phosphatase and is promoted by overexpression of *Sc*Pik1, both of which act on the phosphatidylinositol 4-phosphate [PtdIns(4)*P*] lipid required for Golgi trafficking to the PM (Schorr et al., 2001). Phosphorylation and dephosphorylation also play a role in directing *Sc*Chs3 to the site of septum formation at an appropriate stage of the cell cycle: *Sc*Chs4p is required for the activation of *Sc*Chs3 (Reyes et al., 2007) and to link it to *Sc*Bni4, which interacts with the septin *Sc*Cdc10 at the mother-bud neck (Bulawa, 1993; DeMarini et al., 1997; Reyes et al., 2007); *Sc*Bni4 is phosphorylated at several sites in a cell-cycle-dependent manner (Kozubowski et al., 2003) and recruits the yeast protein phosphatase *Sc*Glc7 to the bud neck, which then facilitates targeting of *Sc*Chs3 to the bud neck (Kozubowski et al., 2003; Larson et al., 2008).

An analysis of the *C. albicans* phospho-proteome revealed that Chs3 can be phosphorylated on the serine residue at position 139 (S139). We constructed strains expressing mutated versions of Chs3 in an attempt to mimic non-phosphorylatable and constitutively phosphorylated forms of Chs3, and found that both phosphorylation and dephosphorylation on S139 are important for Chs3 localisation and function in both yeast and hyphae. Therefore, the regulation of chitin synthase phosphorylation is required for the polarisation of chitin synthesis in cells growing in both yeast and hyphal forms, representing the two major growth forms of fungi.

Results

Chs3 phosphorylation status affects localisation

In a global analysis of the *C. albicans* phospho-proteome using immobilised metal ion affinity chromatography (IMAC) liquid-chromatography tandem mass spectrometry (LC-MS/MS), Chs3 was shown to be phosphorylated on S139 (Fig. 1). Phosphorylation of Chs3 at this site (and five others) was also identified in an independent analysis of the *C. albicans* phospho-proteome by Beltrao et al. (Beltrao et al., 2009). We previously showed that Chs3-YFP is localised at the tips of growing buds and hyphae, and then relocates to the site of septum formation just before cytokinesis (Lenardon et al., 2007) (Fig. 2A). Phosphorylation at S139 might play a role in regulating the localisation of Chs3 in *C. albicans*. We therefore constructed a *chs3*^{S139A} phospho-mutant expressing Chs3 that could not be phosphorylated at S139 (Cheusova et al., 2006; Higashimoto et al., 2007). The Chs3^{S139A} mutant was then C-terminally tagged with YFP (*chs3*^{S139A}*-YFP*). We also constructed a phospho-mutant expressing YFP-tagged Chs3^{S139E} in an attempt to mimic a constitutively phosphorylated form of Chs3 (*chs3*^{S139E}) by inserting a negatively charged amino acid (Cheusova et al., 2006; Higashimoto et al., 2007; Huffine and Scholtz, 1996). The YFP-tagged chitin synthase proteins were detected by western analysis using an antibody against GFP (Lenardon et al., 2007). Both Chs3^{S139A}-YFP and Chs3^{S139E}-YFP were expressed, and no signal was detected in extracts from the untagged strain (BWP17) (Fig. 3A).

In small and medium buds of exponentially growing yeast cells, only 1.8% (*n*=284) of cells had YFP correctly localised at the bud tips in the *chs3*^{S139A}*-YFP* phospho-mutant strain (Fig. 2B). The control *CHS3-YFP* strain showed correct tip localisation in 93.5% (*n*=107) of cells (Fig. 2A). Correct septal localisation was observed in 95.3% (*n*=86) of cells in the G2-M stage of the cell cycle in the *CHS3-YFP* strain (Fig. 2A) compared with only 14.0% (*n*=136) in the *chs3*^{S139A}*-YFP* cells (Fig. 2B). Chs3^{S139E}-YFP was also mislocalised, with correct tip localisation in only 3.3% (*n*=61) of G2 cells and correct septal localisation in 16.7% (*n*=24) of dividing (mitotic) cells (Fig. 2C). These results might indicate that correct localisation of Chs3 requires both phosphorylation and dephosphorylation at S139.

To confirm the sequence of events in the localisation of these proteins, we followed the path of the YFP-tagged versions of Chs3 in growing yeast and hyphal cells embedded in agar by time-lapse microscopy. In yeast cells, Chs3-YFP localised tightly to the tip of small and medium buds, and then relocated to the site of septum formation (Fig. 4A; supplementary material Movies 1 and 2). This pattern of localisation was mimicked in hyphae, where strong fluorescence was observed at the growing tips and developing septa (Fig. 5A; supplementary material Movies 3 and 4). In addition, Chs3-YFP could be seen in small vesicle-like structures being delivered to the growing tip of the hypha (Fig. 5A; supplementary material Movies 3 and 4). No clear pattern of localisation of fluorescence was observed for either YFP-tagged phospho-mutant strain in either yeast (Fig. 4B,C; supplementary

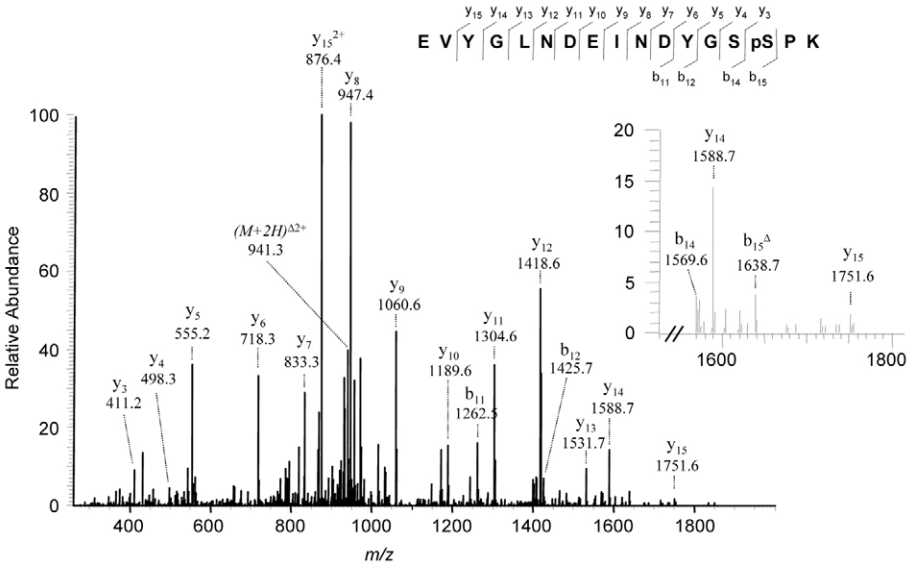

Fig. 1. Identification of a phosphorylation site in Chs3 by MS. Sequencing of the phosphopeptide from Chs3 by nano-electrospray ionisation tandem mass spectrometry (nano-ESI-MS/MS) shows that the serine residue prior to the penultimate proline residue is phosphorylated. $(M+2H)^{\Delta 2+}$ labels the parent ion after the loss of phosphate. The individual y- and b-ions are labelled in the spectra. The inset is a magnified view of a portion of the spectra. The $b_{15}{}^{\Delta}$-ion shows that the serine prior to the proline residue has undergone a neutral loss of phosphate.

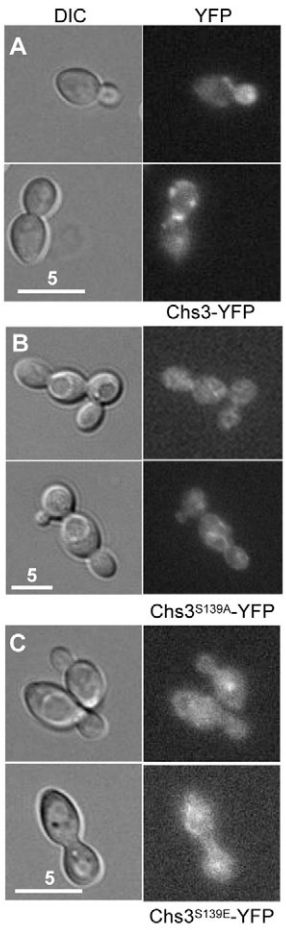

Fig. 2. Phosphorylation at S139 affects Chs3 localisation. (**A**) Chs3-YFP is localised to the tip of growing buds and then relocates to the site of septum formation just before cytokinesis (*CHS3-YFP*). (**B**) Chs3^{S139A}-YFP is mislocalised in the cell (*chs3*^{S139A}). (**C**) Chs3^{S139E}-YFP is also mislocalised (*chs3*^{S139E}). The left panels in each pair show the DIC image and right panels show the corresponding YFP fluorescence. Scale bars: 5 µm.

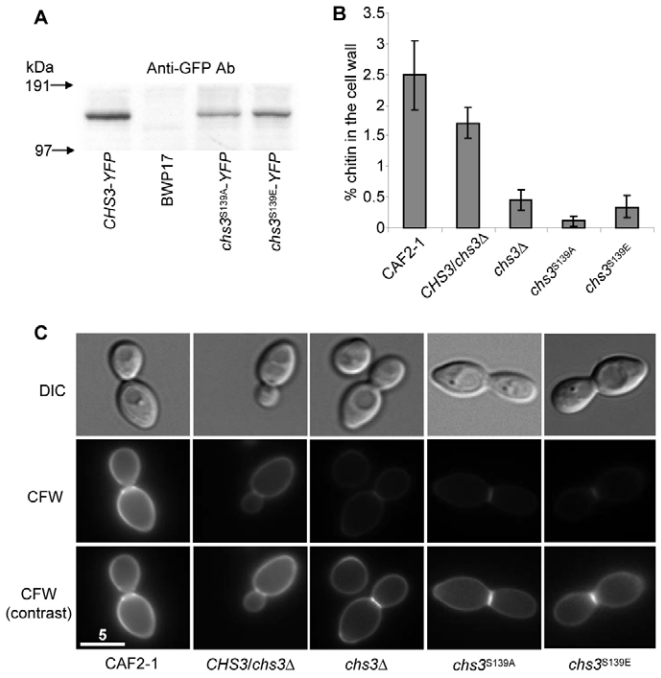

Fig. 3. Expression, cell-wall content and distribution of chitin in Chs3 phospho-mutants. (**A**) Western blot with anti-GFP antibody showing expression of YFP-tagged wild-type and mutant forms of Chs3. Lane 1: Chs3-YFP. Lane 2: untagged negative control. Lane 3: Chs3^{S139A}-YFP. Lane 4: Chs3^{S139E}-YFP. The band corresponding to Chs3-YFP was the only band detected between 97 and 191 kDa. (**B**) The percentage of chitin in the cell walls of the wild type (CAF2-1), *CHS3* heterozygote (*CHS3*/*chs3*Δ), homozygous *chs3*-null mutant (*chs3*Δ) and *chs3* phospho-mutants (*chs3*^{S139A} and *chs3*^{S139E}). We present the average percentage of chitin in the cell-wall dry weight (±s.d.). (**C**) Distribution of chitin in the cell walls of the wild type (CAF2-1), *CHS3* heterozygote (*CHS3*/*chs3*Δ), homozygous *chs3*-null mutant (*chs3*Δ) and *chs3* phospho-mutants (*chs3*^{S139A} and *chs3*^{S139E}) visualised after staining with CFW. Top panels show the DIC reference image. Middle panels show the intensity of CFW fluorescence relative to the wild-type strain. The contrast has been artificially increased in the bottom panels to make the CFW staining visible. Scale bar: 5 µm.

material Movies 5 and 6) or hyphae (Fig. 5B,C; supplementary material Movies 7 and 8).

Chitin synthase phosphorylation affects chitin synthesis

The content and distribution of chitin in the cell walls of the *chs3*^{S139A} and *chs3*^{S139E} strains were similar to those of the *chs3*Δ-null mutant (Fig. 3B). To assess the distribution of chitin, we stained the cells with Calcofluor White (CFW). As shown previously, the intensity of CFW fluorescence accurately represented the amount of chitin in the cell wall (Fig. 3C, middle panels) (Walker et al., 2008). To better visualise the chitin in these cells, we artificially adjusted the contrast of these images (Fig. 3C, bottom panels). The distribution of chitin in the *chs3*^{S139A} and *chs3*^{S139E} strains was similar to that of the *chs3*Δ-null mutant, with the majority of the chitin found in the septal plate rather than the cell walls. Therefore, less chitin was made and deposited in the cell wall when Chs3 could not be phosphorylated or was mutated to mimic constitutive phosphorylation on S139. Therefore, both phosphorylation and dephosphorylation events are important for Chs3 function.

Pkc1 is not required for Chs3 phosphorylation

Two lines of evidence suggested that Pkc1 might phosphorylate Chs3 in *C. albicans*. NetPhosK 1.0 (http://www.cbs.dtu.dk/services/NetPhosK/) predicted that Pkc1 was most likely to phosphorylate Chs3 on S139. In *S. cerevisiae*, *Sc*Chs3 phosphorylation in response to heat stress is dependent on *Sc*Pkc1 (Valdivia and Schekman, 2003).

To test whether Pkc1 was required for phosphorylation of Chs3, we C-terminally tagged Chs3 with YFP in a *pkc1* Tn7-insertion mutant background and observed its localisation by fluorescence microscopy. Time-lapse microscopy of live yeast cells of this strain showed that Chs3-YFP was absent from the tips of growing buds, but did localise to the site of septum formation prior to cytokinesis (Fig. 6A). The same pattern of localisation of Chs3-YFP in this *pkc1* background was also observed in growing hyphae, where diffuse fluorescence was observed at growing tips but strong fluorescence was observed at the site of septum formation (Fig. 6C). Phosphorylation of Chs3 and localisation to sites of polarised growth therefore appeared to be dependent on Pkc1, but Pkc1-dependent phosphorylation was not required to relocate Chs3 to

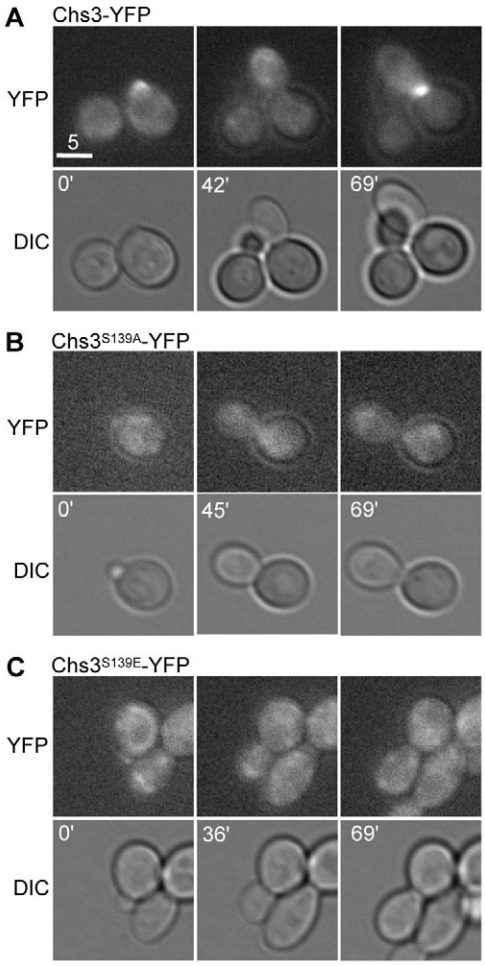

Fig. 4. Localisation of YFP-tagged versions of Chs3 in individual yeast cells. Selected frames of time-lapse videos of (**A**) *CHS3-YFP*, (**B**) *chs3*^{S139A}-*YFP* and (**C**) *chs3*^{S139E}-*YFP* strains growing in the yeast form embedded in agar. Top panels show YFP fluorescence and bottom panels show corresponding DIC images. Scale bar: 5 µm. Numbers on the DIC images represent the elapsed time in minutes. Video clips of selected cells showing 3 minute frames over one complete cell division cycle are available as supplementary material. *CHS3-YFP*: supplementary material Movie 1 (YFP) and supplementary material Movie 2 (DIC); *chs3*^{S139A}-*YFP*: supplementary material Movie 5 (YFP) and supplementary material Movie 6 (DIC).

the site of septum formation. However, genotypic analysis of the *pkc1* Tn7-insertion mutant using the PCR-based method described in Enloe et al. (primers Pkc1amp5, Pkc1amp3 and Arg4det; supplementary material Table S1) revealed that, in addition to two *pkc1* mutant alleles (*pkc1*::Tn7-*UAU1* and *pkc1*::Tn7-*URA3*), a third wild-type copy of *PKC1* was also present in this strain (Enloe et al., 2000). We therefore renamed this strain *pkc1*/*pkc1*/*PKC1* (supplementary material Table S2).

To assess whether the phenotype observed above was related to *PKC1*, we constructed a true *pkc1*Δ-null mutant strain (*pkc1*Δ; supplementary material Table S2) and C-terminally tagged Chs3 with YFP in this strain (*pkc1*Δ *CHS3-YFP*; supplementary material Table S2). Time-lapse microscopy of live yeast (Fig. 6B) and hyphal (Fig. 6D) cells showed that the localisation of Chs3-YFP in the *pkc1*Δ-null mutant was identical to the localisation of Chs3-YFP in a wild-type background (Fig. 4A, Fig. 5A). Therefore, Pkc1 is not required for Chs3 phosphorylation during the conditions used to examine yeast and hyphal growth.

Discussion

We have shown that Chs3 phosphorylation and dephosphorylation on S139 are crucial for the accurate polarisation of this protein during the cell cycle. Both a non-phosphorylatable form and a form of Chs3 mutated to mimic phosphorylation at S139 are expressed, but are mislocalised in both yeast and hyphal cells. In *S. cerevisiae*, *Sc*Chs3 is transported from the ER to Golgi to the PM by specific chaperones *Sc*Chs7, *Sc*Chs5, *Sc*Chs6 and *Sc*Chs4 (Sanchatjate and Schekman, 2006; Santos and Snyder, 1997; Trautwein et al., 2006; Trilla et al., 1999; Ziman et al., 1996; Ziman et al., 1998). The inability to phosphorylate Chs3 did not prevent the transport of Chs3 from the ER, as no colocalisation of Chs3^{S139A}-YFP was observed with an ER stain (data not shown). In some images, particularly of hyphal cells, the YFP-tagged phospho-mutant forms of Chs3 formed long string-like structures with an arrangement that resembled axial microtubules. However, we found no evidence that Chs3 was associated with microtubules. Chs3-YFP localised normally in the presence of an inhibitory concentration of benomyl, a drug that inhibits microtubule polymerisation (data not shown). Also, Chs3-YFP did not coimmunoprecipitate with tubulin or actin (data not shown).

*C. albicans chs3*Δ cells have significantly reduced cell-wall chitin, and the level and distribution of chitin in the cell wall of *chs3*^{S139A} and *chs3*^{S139E} cells were similar to that seen in the *chs3*Δ-null mutant. This could be interpreted to mean that both phosphorylation and dephosphorylation of Chs3 on S139 are important for the correct localisation and function of Chs3 throughout the cell cycle. However, if the S139E mutation did not mimic constitutive phosphorylation at this site, then both the S139A and S139E mutations would produce a non-phosphorylatable form of Chs3. In this case, this might suggest that only phosphorylation of Chs3 on S139 is required for the correct localisation and function of Chs3.

Analysis of the Chs3 protein sequence using NetPhos 2.0 (http://www.cbs.dtu.dk/services/NetPhos/) predicted that phosphorylation is likely on 43 serine residues, 16 threonine residues and 18 tyrosine residues spread over the entire protein sequence. Phosphorylation of Chs3 was only detected on S139 in our IMAC LC-MS/MS analysis, which we have shown to be biologically relevant. Martinez-Rucobo et al. identified twelve biologically relevant phosphorylation sites in the N terminus of *Sc*Chs2 by IMAC LC-MS/MS (Martinez-Rucobo et al., 2009). These included six sites not predicted by NetPhos 2.0. *Sc*Chs2 is the functional homologue of *Ca*Chs1 (Munro et al., 2001), a class II chitin synthase, and is expressed, localised and degraded in a cell-cycle-dependent manner (Roncero, 2002). Deletion of the N-terminal region of *Sc*Chs2 containing the twelve phosphorylation sites resulted in degradation of *Sc*Chs2 (Martinez-Rucobo et al., 2009). Four of the twelve phosphorylation sites matched the consensus phosphorylation sequence for *Sc*Cdk1 (cyclin-dependent kinase 1), indicating a possible mechanism for phosphorylation in the turnover of this protein at appropriate stages of the cell cycle (Martinez-Rucobo et al., 2009).

Our data suggest that polarisation of Chs3 to growing tips is dependent on S139 phosphorylation early in the cell cycle. This is supported by the observation that Chs3^{S139A}-YFP fails to localise to growing tips. If the S139E mutation does mimic constitutive phosphorylation at this site, then a dephosphorylation event must

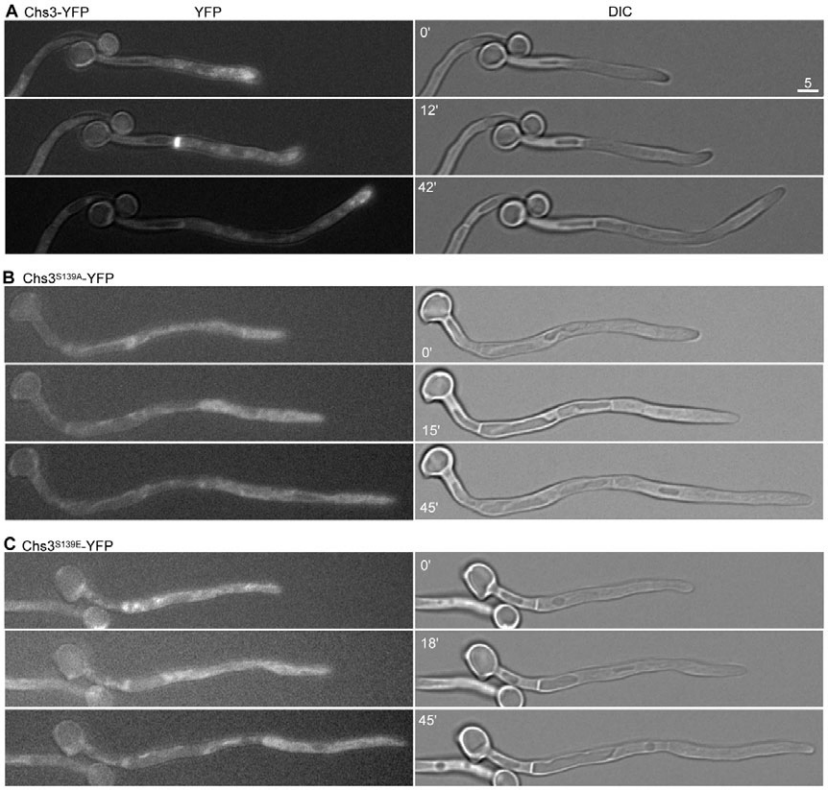

Fig. 5. Time-lapse images of YFP-tagged versions of Chs3 in growing hyphae. Selected frames of (**A**) *CHS3-YFP*, (**B**) *chs3*^{S139A}*-YFP* and (**C**) *chs3*^{S139E}*-YFP* strains grown under hypha-forming conditions embedded in agar. Left panels show YFP fluorescence and right panels show corresponding DIC images. Scale bar: 5 µm. Numbers on the DIC images represent the elapsed time in minutes. Video clips showing 3 minute frames of growing hyphae are available as supplementary material. *CHS3-YFP*: supplementary material Movie 3 (YFP) and supplementary material Movie 4 (DIC); *chs3*^{S139A}*-YFP*: supplementary material Movie 7 (YFP) and supplementary material Movie 8 (DIC).

occur to allow Chs3 to remain at the tip of growing buds and hyphae. Relocation events that target Chs3 to the mother-bud neck prior to cytokinesis might also involve phosphorylation. In only a small proportion of dividing cells did both Chs3 phospho-mutant forms reach the site of septum formation (14% for Chs3^{S139A}-YFP and 16.7% for Chs3^{S139E}-YFP). Transient phosphorylation of Chs3 on S139 might therefore allow or prevent interaction with other proteins that recruit Chs3 to the appropriate sites in the cell, at the appropriate time in the cell cycle.

An interesting phenotype with respect to Chs3-YFP localisation was observed in the *pkc1*/*pkc1*/*PKC1* mutant. This phenotype was not a result of a *PKC1*-gene dosage effect, because the same or

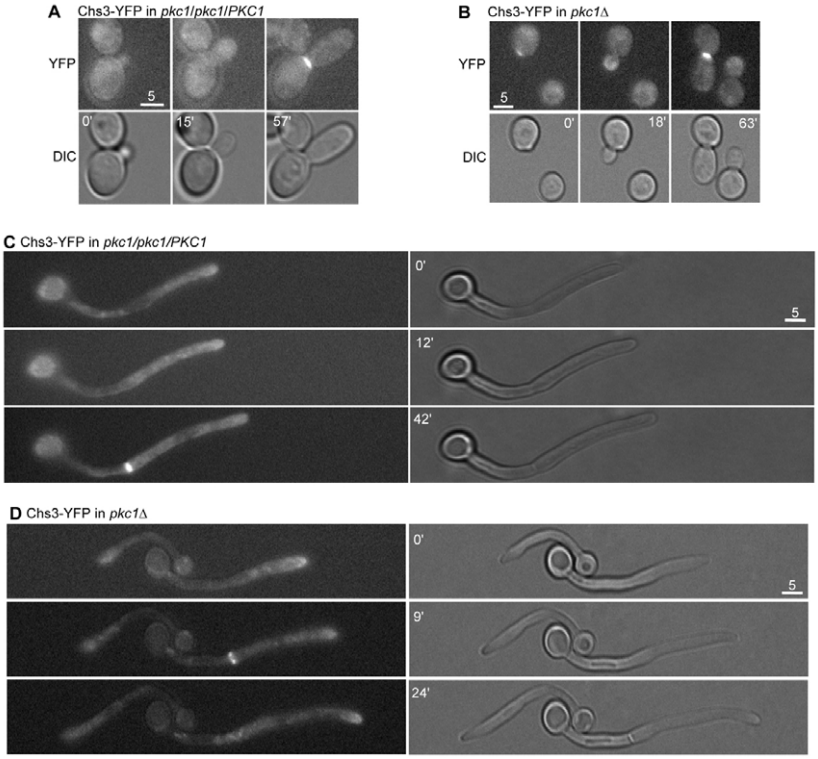

Fig. 6. Localisation of Chs3-YFP in *pkc1* mutant strains. Selected frames of time-lapse videos of (**A**) *pkc1*/*pkc1*/*PCK1 CHS3-YFP* and (**B**) *pkc1*Δ *CHS3-YFP* strains growing in the yeast form embedded in agar. Selected frames of the (**C**) *pkc1*/*pkc1*/*PKC1 CHS3-YFP* and (**D**) *pkc1*Δ *CHS3-YFP* strains grown under hypha-forming conditions embedded in agar. Left panels show YFP fluorescence and right panels show corresponding DIC images. Scale bars: 5 µm. Numbers on the DIC images represent the elapsed time in minutes.

Journal of Cell Science

even similar phenotype was not observed in the *pkc1*Δ-null mutant. *PKC1* is located on chromosome 3. A quick assessment of the karyotype of the *pkc1*/*pkc1*/*PKC1* mutant using the multiplex-PCR-based method described by Arbour et al. (Arbour et al., 2009) revealed that the third copy of *PKC1* in this strain had not been created by a simple duplication of chromosome 3 (data not shown). Instead, the *pkc1*/*pkc1*/*PKC1* mutant contained an extra copy of chromosome 6, chromosome 7 and part of the right arm of chromosome 5, compared with its parent strain (BWP17). This strongly indicates that some other genetic abnormality in this strain is the cause of the mislocalisation of Chs3-YFP.

The sequence surrounding the mapped phosphorylation site at S139 is a consensus cyclin-dependent kinase (CDK) phosphorylation site (S/T-P-X-K/R) (Endicott et al., 1999). *C. albicans* has a single CDK, Cdc28, which interacts with the B-type cyclin Clb2 (Cyb1) to regulate the G2-M transition (Damagnez and Cottarel, 1996). Cdc28 is inhibited when phosphorylated by Swe1, which in turn is negatively regulated by the kinase Hsl1, forming an Hsl1-Swe1-Cdc28 regulatory pathway thought to control cell elongation in both yeast and hyphal forms (Umeyama et al., 2005). Hsl1-GFP and septins colocalise in yeast and hyphal cells, and Hsl1 appears to be active only when colocalised with the septins (Umeyama et al., 2005). This implies that Cdc28 would be active early in the cell cycle, when Chs3 S139 is phosphorylated and localised to growing tips. The possibility that Cdc28 is the kinase that phosphorylates Chs3 on S139 is under investigation in our laboratory. Although the kinase responsible for phosphorylation of Chs3 on S139 is currently unknown, this work has demonstrated for the first time that phosphorylation regulates polarisation of chitin synthesis in *C. albicans*.

Materials and Methods

Strains, media and growth conditions

The *C. albicans* strains used in this work are all congenic (supplementary material Table S2). They were grown at 30°C in liquid-rich medium (YEPD+Uri) containing 1% yeast extract, 2% mycopeptone and 2% glucose supplemented with 25 μg/ml uridine. Transformants were selected and maintained on minimal medium (SD) containing 0.67% yeast nitrogen base with ammonium sulfate, 2% glucose and appropriate supplements. *E. coli* strain XL-10 Gold (Stratagene) used in this work was grown on Luria-Bertani (LB) medium containing 0.5% yeast extract, 1% tryptone and 1% NaCl supplemented with 100 μg/ml ampicillin.

Phosphopeptide preparation

Proteins precipitated by acetone were resuspended in 50 mM ammonium bicarbonate with 0.05% Rapigest (Waters) and phosphatase inhibitors. Proteins were digested with trypsin (Promega) overnight, lyophilised and dissolved in 5 mM ammonium formate buffer, pH 2.7. Tryptic peptides were run on a strong cation-exchange column (SCX; polysulfoethylaspartamide column size: 200×3.2 mm, 3.5 μm, 200 Å; PolyLC, Columbia, USA) to fractionate the sample. 1 ml high-performance liquid chromatography (HPLC) fractions were collected, lyophilised, then dissolved in 10% acetic acid and run through an IMAC column (Ga^{3+}) to enrich for phosphopeptides. IMAC eluates were lyophilised and redissolved in 1% acetonitrile, 0.1% formic acid for analysis by mass spectrometry (MS).

Mass spectrometry

LC-MS/MS analysis was performed using a LTQ mass spectrometer (Thermo Electron, San Jose, CA, USA) and a nanoflow-HPLC system (Surveyor, Thermo Electron). Peptides were applied to a precolumn (C18 pepmap100; LC Packings) connected to a self-packed C18 8-cm analytical column (BioBasic resin Thermo Electron; Picotip 75 μm id, 15 μm tip, New Objective). Peptides were eluted by a gradient of 2-60% acetonitrile in 0.1% formic acid over 50 minutes at a flow rate of approximately 250 nl/minute. Data-dependent acquisition of MS/MS consisted of selection of the six most abundant ions in each cycle: MS mass-to-charge ratio (*m*/*z*) 300 to 2000, minimum signal 1000, collision energy 28, 5 repeat hits, 300 s exclusion. MS3 were triggered if the neutral loss of phosphoric acid (49 *m*/*z* for 2+ parent ions) was detected in the three most abundant ions on the preceding MS2. Collision energy for MS3 was 35. In all cases, the mass spectrometer was operated in positive-ion mode with a nanospray source and a capillary temperature of 200°C; no sheath gas was employed and the source and focusing voltages were optimised for the transmission of angiotensin.

Raw data were processed using BioWorks 3.2 and TurboSEQUEST (Thermo Electron), and searched against CandidaDB (http://genolist.pasteur.fr/CandidaDB/), a database dedicated to the analysis of the genome *C. albicans*, with the following variable modifications: oxidised methionine and phosphorylated serine or threonine. Peptide hits were filtered by Xcorr and charge state [Xc (+1, 2, 3) 2.0, 2.5, 3.5], with one missed tryptic cleavage allowed. MS2 and MS3 data were searched separately. All peptides passing the basic threshold criteria of Xcorr were verified manually for the presence of b- and y-ion series associated with phosphorylation of the peptide.

Construction of plasmids and phospho-mutant strains

C. albicans strains that express mutant forms of Chs3 were constructed by reintroducing one copy of the mutant *chs3* alleles at the native chromosomal locus in a *chs3*Δ-null mutant strain. To facilitate integration by homologous recombination and recycling of the *URA3* selective marker, the *CHS3* promoter, *CHS3* open reading frame (ORF), *CHS3* terminator, *URA3* and a second copy of the *CHS3* terminator were cloned between the *Not*I and *Apa*I sites in the plasmid pBluescript SK+ (Stratagene). Plasmid pBS-URA3 was generated by excising the *URA3* gene from plasmid pDBV51 (Brown et al., 1996) with *Sca*I and *Sal*I, and inserting it between the *Sma*I and *Xba*I sites of pBluescript SK+. The promoter, ORF and terminator of the *CHS3* gene (–267 to +4135 relative to ATG^{CHS3}) were amplified by PCR using the primers CHS3Ia and CHS3IIb (supplementary material Table S1), which introduced a *Not*I and *Xba*I site at each end. Similarly, the *CHS3* terminator (+3643 to +4345 relative to ATG^{CHS3}) was amplified using the primers CHS3IIIa and CHS3IIIb (supplementary material Table S1), which introduced a *Sal*I and *Apa*I site at each end. The two PCR products were then ligated between the *Not*I and *Xba*I sites, and the *Sal*I and *Apa*I sites, respectively, of pBS-URA3 to generate the plasmid pBS-CHS3-3.

Specific mutations of the *CHS3* ORF in the plasmid pBSCHS3-3 were created by site-directed mutagenesis using the QuikChange II XL site-directed mutagenesis kit (Stratagene) as per the manufacturer's instructions. The serine to alanine mutation was introduced by changing TCA at position +415 in the *CHS3* ORF (relative to ATG^{CHS3}) to GCA using the mutagenic oligonucleotide primers SM1 and SM2 (supplementary material Table S1). Similarly, the serine to glutamic acid mutation was introduced by changing TCA to GAA using the mutagenic oligonucleotide primers MDL90 and MDL91 (supplementary material Table S1). Mutations were confirmed by DNA sequencing before proceeding.

The *Not*I and *Apa*I cassettes from pBSCHS3-3(S139A) and pBSCHS3-3(S139E) were transformed into the *C. albicans chs3*Δ-null mutant strain (supplementary material Table S2). The homologous promoter and terminator regions targeted the integration of the cassette to the native *CHS3* locus. Ura^+ transformants were selected and correct integration at the *CHS3* locus was confirmed by Southern analysis. Transformants with correctly integrated cassettes were subjected to 5-fluorootic acid (5-FOA) selection. Ura^- colonies were selected and loss of the *URA3* gene was confirmed by Southern analysis. The preservation of the mutations introduced into the *CHS3* ORF was confirmed by DNA sequencing following integration into the *C. albicans* chromosome at both the pre- and post-FOA stages, thus confirming the successful construction of the strains $chs3^{S139A}$ and $chs3^{S139E}$ (supplementary material Table S2).

Construction of a *pkc1*Δ-null mutant

A *pkc1*Δ-null mutant was constructed by sequentially deleting both copies of the entire *PKC1* ORF using the mini-Ura-blaster method (Wilson et al., 2000). The *URA3-dpl200* cassette, with 100 base pair homology to the sequence immediately flanking each end of the *PKC1* ORF, was amplified from pDDB57 (Wilson et al., 2000) using primers MDL230 and MDL231 (supplementary material Table S1). The resulting *pkc1::dpl200-URA3-dpl200* cassette was transformed into *C. albicans* strain BWP17 (supplementary material Table S2). Ura^+ transformants were selected and integration of the mini-Ura-blaster cassette at the *PKC1* locus was confirmed by PCR (primers MDL232 and MDL183; supplementary material Table S1). Transformants with correctly integrated cassettes were subjected to 5-FOA selection. Ura^- colonies were selected and the loss of the *URA3* gene was confirmed by PCR (primers MDL232 and MDL233; supplementary material Table S1). The process was repeated to delete the second copy of *PKC1*, creating strain *pkc1*Δ (supplementary material Table S2). The absence of the *PKC1* gene was also confirmed by PCR (primers Pkc1amp5 and Pkc1amp3; supplementary material Table S1).

Construction of YFP-tagged strains

The phospho-mutant versions of *CHS3* in the $chs3^{S139A}$ and $chs3^{S139E}$ strains (supplementary material Table S2), and one copy of *CHS3* in the *pkc1*Δ-null mutant (supplementary material Table S2) were fused to the gene encoding YFP using the method described by Gerami-Nejad et al. (Gerami-Nejad et al., 2001). Briefly, PCR primers with 100 base pair homology to the sequence immediately upstream and downstream of the stop codon of *CHS3* were designed to anneal to either end of the YFP cassette in the plasmid pYFP-URA3 (Gerami-Nejad et al., 2001) (primers MDL5 and MDL6; supplementary material Table S1). The resulting PCR product containing *YFP*, the *ADH1* terminator sequence and the *URA3* marker gene was transformed into the $chs3^{S139A}$ and $chs3^{S139E}$ strains (supplementary material Table

Journal of Cell Science

S2). Ura$^+$ colonies were screened for the presence of the correctly integrated YFP cassette by Southern analysis and by PCR (primers MDL40 and MDL16R; supplementary material Table S1), thus confirming the successful construction of the strains *chs3*^{S139A}*-YFP*, *chs3*^{S139E}*-YFP* and *pkc1*Δ *CHS3-YFP* (supplementary material Table S2).

One copy of the *CHS3* gene was tagged with *YFP* in the *pkc1*/*pkc1*/*PKC1* mutant strain using a similar strategy. PCR primers with 100 base pair homology to the sequence immediately upstream and downstream of the stop codon of *CHS3* were designed to anneal to either end of the YFP cassette in the plasmid pYFP-HIS1 (Gerami-Nejad et al., 2001) (primers MDL5 and MDL81; supplementary material Table S1). The resulting PCR product containing *YFP*, the *ADH1* terminator sequence and the *HIS1* marker gene was transformed into the *pkc1*Δ strain (supplementary material Table S2). His$^+$ colonies were screened for the presence of the correctly integrated YFP cassette by Southern analysis.

Microscopy

To visualise large numbers of live yeast cells, YFP-tagged strains were grown in liquid YEPD+Uri for 4 h at 30°C with shaking at 200 rpm. Samples were harvested, washed in PBS and mounted on a slide under a coverslip. Cells were visualised using a DeltaVision Core microscope (Applied Precision) equipped with a CoolSNAP camera (Photometrics). YFP fluorescence was detected using a standard fluorescein isothiocyanate (FITC) filter set.

Time-lapse movies of growing yeast and hyphal cells were made using a method similar to that of Veses and Gow (Veses and Gow, 2008). Yeast cells from an overnight culture were inoculated on the surface of an agar pad filling the cavity of a glass cavity slide (Agar Scientific), covered with a coverslip, and sealed using a mixture of lanoline, Vaseline and paraffin wax (1:1:1). For movies of yeast cells, the agar pad was made from rich media (SC) containing 0.67% yeast nitrogen base with ammonium sulfate, 0.2% complete amino acid mix, 2% glucose and 1.2% purified agar. For movies of hyphal cells, the agar pad consisted of 20% FCS and 1.2% purified agar. Slides were incubated in the environmental chamber surrounding the microscope at 30°C or 37°C for movies of yeast or hyphal cells, respectively. A differential interference contrast (DIC) and YFP fluorescent image was taken every 3 minutes for the duration of the movies.

To observe the distribution of chitin in the cells, cells were mounted on a slide under a coverslip with 1 µl of a 10 µg/ml solution of CFW. CFW stain was detected using a standard DAPI filter set.

Western analysis of Chs3

Chs3 expression was analysed by western blotting as described in Walker et al. (Walker et al., 2008). Proteins were prepared from 50 ml cultures of yeast cells grown in YEPD+Uri at 30°C for 4 hours with shaking at 200 rpm.

Measurement of cell-wall chitin

Chitin content was measured for cells grown in 200 ml YEPD+Uri for 4 hours at 30°C with shaking at 200 rpm. The chitin content of the cell wall was determined as described in Plaine et al. (Plaine et al., 2008).

In silico analyses

Prediction of Chs3 phosphorylation sites was performed with NetPhos 2.0 (http://www.cbs.dtu.dk/services/NetPhos/) and kinase predictions were made with NetPhosK 1.0 (http://www.cbs.dtu.dk/services/NetPhosK/).

We thank Serena Selvaggini, Aaron Mitchell, Laura Selway and Claire Walker for strains and ancillary information, and the Wellcome Trust, BBSRC, EC (FUNGWALL) and MRC for funding. Deposited in PMC for immediate release. This article is freely accessible online from the date of publication.

Supplementary material available online at
http://jcs.biologists.org/cgi/content/full/123/13/2199/DC1

References

Arbour, M., Epp, E., Hogues, H., Sellam, A., Lacroix, C., Rauceo, J., Mitchell, A., Whiteway, M. and Nantel, A. (2009). Widespread occurrence of chromosomal aneuploidy following the routine production of *Candida albicans* mutants. *FEMS Yeast Res.* **9**, 1070-1077.

Bartnicki-Garcia, S. (2006). Chitosomes: past, present and future. *FEMS Yeast Res.* **6**, 957-965.

Beltrao, P., Trinidad, J. C., Fiedler, D., Roguev, A., Lim, W. A., Shokat, K. M., Burlingame, A. L. and Krogan, N. J. (2009). Evolution of phosphoregulation: comparison of phosphorylation patterns across yeast species. *PLoS Biol.* **7**, e1000134.

Brown, D. H., Jr, Slobodkin, I. V. and Kumamoto, C. A. (1996). Stable transformation and regulated expression of an inducible reporter construct in *Candida albicans* using restriction enzyme-mediated integration. *Mol. Gen. Genet.* **251**, 75-80.

Bulawa, C. E. (1993). Genetics and molecular biology of chitin synthesis in fungi. *Annu. Rev. Microbiol.* **47**, 505-534.

Bulawa, C. E., Miller, D. W., Henry, L. K. and Becker, J. M. (1995). Attenuated virulence of chitin-deficient mutants of *Candida albicans*. *Proc. Natl. Acad. Sci. USA* **92**, 10570-10574.

Cheusova, T., Khan, M. A., Schubert, S. W., Gavin, A. C., Buchou, T., Jacob, G., Sticht, H., Allende, J., Boldyreff, B., Brenner, H. R. et al. (2006). Casein kinase 2-dependent serine phosphorylation of MuSK regulates acetylcholine receptor aggregation at the neuromuscular junction. *Genes Dev.* **20**, 1800-1816.

Choi, W. J., Sburlati, A. and Cabib, E. (1994). Chitin synthase 3 from yeast has zymogenic properties that depend on both the *CAL1* and the *CAL3* genes. *Proc. Natl. Acad. Sci. USA* **91**, 4727-4730.

Chuang, J. S. and Schekman, R. W. (1996). Differential trafficking and timed localization of two chitin synthase proteins, Chs2p and Chs3p. *J. Cell Biol.* **135**, 597-610.

Damagnez, V. and Cottarel, G. (1996). *Candida albicans CDK1* and *CYB1*: cDNA homologues of the *cdc2*/*CDC28* and *cdc13*/*CLB1*/*CLB2* cell cycle control genes. *Gene* **172**, 137-141.

Davis, D. A., Bruno, V. M., Loza, L., Filler, S. G. and Mitchell, A. P. (2002). *Candida albicans* Mds3p, a conserved regulator of pH responses and virulence identified through insertional mutagenesis. *Genetics* **162**, 1573-1581.

DeMarini, D. J., Adams, A. E., Fares, H., De Virgilio, C., Valle, G., Chuang, J. S. and Pringle, J. R. (1997). A septin-based hierarchy of proteins required for localized deposition of chitin in the *Saccharomyces cerevisiae* cell wall. *J. Cell Biol.* **139**, 75-93.

Endicott, J. A., Noble, M. E. and Tucker, J. A. (1999). Cyclin-dependent kinases: inhibition and substrate recognition. *Curr. Opin. Struct. Biol.* **9**, 738-744.

Enloe, B., Diamond, A. and Mitchell, A. P. (2000). A single-transformation gene function test in diploid *Candida albicans*. *J. Bacteriol.* **182**, 5730-5736.

Fischer, R., Zekert, N. and Takeshita, N. (2008). Polarized growth in fungi-interplay between the cytoskeleton, positional markers and membrane domains. *Mol. Microbiol.* **68**, 813-826.

Fonzi, W. A. and Irwin, M. Y. (1993). Isogenic strain construction and gene mapping in *Candida albicans*. *Genetics* **134**, 717-728.

Gerami-Nejad, M., Berman, J. and Gale, C. A. (2001). Cassettes for the PCR-mediated construction of green, yellow, and cyan fluorescent protein fusions in *Candida albicans*. *Yeast* **18**, 859-864.

Gow, N. A. R., Robbins, P. W., Lester, J. W., Brown, A. J., Fonzi, W. A., Chapman, T. and Kinsman, O. S. (1994). A hyphal-specific chitin synthase gene (*CHS2*) is not essential for growth, dimorphism, or virulence of *Candida albicans*. *Proc. Natl. Acad. Sci. USA* **91**, 6216-6220.

Higashimoto, K., Kuhn, P., Desai, D., Cheng, X. and Xu, W. (2007). Phosphorylation-mediated inactivation of coactivator-associated arginine methyltransferase 1. *Proc. Natl. Acad. Sci. USA* **104**, 12318-12323.

Huffine, M. E. and Scholtz, J. M. (1996). Energetic implications for protein phosphorylation. Conformational stability of HPr variants that mimic phosphorylated forms. *J. Biol. Chem.* **271**, 28898-28902.

Kozubowski, L., Panek, H., Rosenthal, A., Bloecher, A., DeMarini, D. J. and Tatchell, K. (2003). A Bni4-Glc7 phosphatase complex that recruits chitin synthase to the site of bud emergence. *Mol. Biol. Cell* **14**, 26-39.

Larson, J. R., Bharucha, J. P., Ceaser, S., Salamon, J., Richardson, C. J., Rivera, S. M. and Tatchell, K. (2008). Protein phosphatase type 1 directs chitin synthesis at the bud neck in *Saccharomyces cerevisiae*. *Mol. Biol. Cell* **19**, 3040-3051.

Lenardon, M. D., Whitton, R. K., Munro, C. A., Marshall, D. and Gow, N. A. R. (2007). Individual chitin synthase enzymes synthesize microfibrils of differing structure at specific locations in the *Candida albicans* cell wall. *Mol. Microbiol.* **66**, 1164-1173.

Lenardon, M. D., Lesiak, I., Munro, C. A. and Gow, N. A. R. (2009). Dissection of the *Candida albicans* class I chitin synthase promoters. *Mol. Genet. Genomics* **281**, 459-471.

Martinez-Rucobo, F. W., Eckhardt-Strelau, L. and Terwisscha van Scheltinga, A. C. (2009). Yeast chitin synthase 2 activity is modulated by proteolysis and phosphorylation. *Biochem. J.* **417**, 547-554.

Merzendorfer, H. (2006). Insect chitin synthases: a review. *J. Comp. Physiol. B Biochem. Syst. Environ. Physiol.* **176**, 1-15.

Mio, T., Yabe, T., Sudoh, M., Satoh, Y., Nakajima, T., Arisawa, M. and Yamada-Okabe, H. (1996). Role of three chitin synthase genes in the growth of *Candida albicans*. *J. Bacteriol.* **178**, 2416-2419.

Munro, C. A. and Gow, N. A. R. (2001). Chitin synthesis in human pathogenic fungi. *Med. Mycol.* **1**, 41-53.

Munro, C. A., Schofield, D. A., Gooday, G. W. and Gow, N. A. R. (1998). Regulation of chitin synthesis during dimorphic growth of *Candida albicans*. *Microbiology* **144**, 391-401.

Munro, C. A., Winter, K., Buchan, A., Henry, K., Becker, J. M., Brown, A. J., Bulawa, C. E. and Gow, N. A. R. (2001). Chs1 of *Candida albicans* is an essential chitin synthase required for synthesis of the septum and for cell integrity. *Mol. Microbiol.* **39**, 1414-1426.

Munro, C. A., Whitton, R. K., Hughes, H. B., Rella, M., Selvaggini, S. and Gow, N. A. R. (2003). *CHS8*-a fourth chitin synthase gene of *Candida albicans* contributes to in vitro chitin synthase activity, but is dispensable for growth. *Fungal Genet. Biol.* **40**, 146-158.

Munro, C. A., Selvaggini, S., de Bruijn, I., Walker, L., Lenardon, M. D., Gerssen, B., Milne, S., Brown, A. J. and Gow, N. A. R. (2007). The PKC, HOG and Ca^{2+} signalling pathways co-ordinately regulate chitin synthesis in *Candida albicans*. *Mol. Microbiol.* **63**, 1399-1413.

Plaine, A., Walker, L., Da Costa, G., Mora-Montes, H. M., McKinnon, A., Gow, N. A. R., Gaillardin, C., Munro, C. A. and Richard, M. L. (2008). Functional analysis of *Candida albicans* GPI-anchored proteins: Roles in cell wall integrity and caspofungin sensitivity. *Fungal Genet. Biol.* **45**, 1404-1414.

Reyes, A., Sanz, M., Duran, A. and Roncero, C. (2007). Chitin synthase III requires Chs4p-dependent translocation of Chs3p into the plasma membrane. *J. Cell Sci.* **120**, 1998-2009.

Roncero, C. (2002). The genetic complexity of chitin synthesis in fungi. *Curr. Genet.* **41**, 367-378.

Sanchatjate, S. and Schekman, R. (2006). Chs5/6 complex: a multiprotein complex that interacts with and conveys chitin synthase III from the trans-Golgi network to the cell surface. *Mol. Biol. Cell* **17**, 4157-4166.

Santos, B. and Snyder, M. (1997). Targeting of chitin synthase 3 to polarized growth sites in yeast requires Chs5p and Myo2p. *J. Cell Biol.* **136**, 95-110.

Schorr, M., Then, A., Tahirovic, S., Hug, N. and Mayinger, P. (2001). The phosphoinositide phosphatase Sac1p controls trafficking of the yeast Chs3p chitin synthase. *Curr. Biol.* **11**, 1421-1426.

Sudoh, M., Nagahashi, S., Doi, M., Ohta, A., Takagi, M. and Arisawa, M. (1993). Cloning of the chitin synthase 3 gene from *Candida albicans* and its expression during yeast-hyphal transition. *Mol. Gen. Genet.* **241**, 351-358.

Trautwein, M., Schindler, C., Gauss, R., Dengjel, J., Hartmann, E. and Spang, A. (2006). Arf1p, Chs5p and the ChAPs are required for export of specialized cargo from the Golgi. *EMBO J.* **25**, 943-954.

Trilla, J. A., Duran, A. and Roncero, C. (1999). Chs7p, a new protein involved in the control of protein export from the endoplasmic reticulum that is specifically engaged in the regulation of chitin synthesis in *Saccharomyces cerevisiae*. *J. Cell Biol.* **145**, 1153-1163.

Umeyama, T., Kaneko, A., Nagai, Y., Hanaoka, N., Tanabe, K., Takano, Y., Niimi, M. and Uehara, Y. (2005). *Candida albicans* protein kinase CaHsl1p regulates cell elongation and virulence. *Mol. Microbiol.* **55**, 381-395.

Valdivia, R. H. and Schekman, R. (2003). The yeasts Rho1p and Pkc1p regulate the transport of chitin synthase III (Chs3p) from internal stores to the plasma membrane. *Proc. Natl. Acad. Sci. USA* **100**, 10287-10292.

Veses, V. and Gow, N. A. R. (2008). Vacuolar dynamics during the morphogenetic transition in *Candida albicans*. *FEMS Yeast Res.* **8**, 1339-1348.

Walker, L. A., Munro, C. A., de Bruijn, I., Lenardon, M. D., McKinnon, A. and Gow, N. A. R. (2008). Stimulation of chitin synthesis rescues *Candida albicans* from echinocandins. *PLoS Pathog.* **4**, e1000040.

Wilson, R. B., Davis, D. and Mitchell, A. P. (1999). Rapid hypothesis testing with *Candida albicans* through gene disruption with short homology regions. *J. Bacteriol.* **181**, 1868-1874.

Wilson, R. B., Davis, D., Enloe, B. M. and Mitchell, A. P. (2000). A recyclable *Candida albicans URA3* cassette for PCR product-directed gene disruptions. *Yeast* **16**, 65-70.

Ziman, M., Chuang, J. S. and Schekman, R. W. (1996). Chs1p and Chs3p, two proteins involved in chitin synthesis, populate a compartment of the *Saccharomyces cerevisiae* endocytic pathway. *Mol. Biol. Cell* **7**, 1909-1919.

Ziman, M., Chuang, J. S., Tsung, M., Hamamoto, S. and Schekman, R. (1998). Chs6p-dependent anterograde transport of Chs3p from the chitosome to the plasma membrane in *Saccharomyces cerevisiae*. *Mol. Biol. Cell* **9**, 1565-1576.

Journal of Cell Science